Area-Creep Measurements for Crystalline Monolayer of Stearic Acid on the Water Surface

Taishi KURI, Yushi OISHI, and Tisato KAJIYAMA*
Department of Chemical Science and Technology, Faculty of Engineering, Kyushu University, 6-10-1 Hakozaki, Higashi-ku, Fukuoka 812

(Received October 1, 1993)

The area-creep mechanism for the crystalline monolayer of stearic acid on the water surface was discussed on the basis of area-creep measurements and transmission electron microscopic observations. The area-creep behaviors of the crystalline monolayer at a high surface pressure region ($\geq$15 mN m^{-1}) was apparently different from those at a low one ($\leq$10 mN m^{-1}). At a high surface pressure region, the area-creep behavior of the monolayer was mainly classified into the two processes in shorter and longer creep time regions with respect to around 1×10^2 s. The area strain in a short creep time region was small and increased linearly with the creep time, that might be attributed to rearrangement of molecules in the crystalline monolayer during the area-creep (molecular creep). On the other hand, the area strain in a long creep time region increased remarkably owing to collapse of the monolayer (geometrical aggregation creep). Also at a low surface pressure region, the area strain was small and became almost constant at around 1×10^4 s after the area-creep experiment started. In the case of the area-creep of the crystalline monolayer at a low surface pressure, rearrangement of molecules in the crystalline monolayer and/or filling in vacancies of molecular level in the interfacial regions among the crystalline monolayer domains were proceeded with a creep time, and then, the crystallographical regularity in the monolayer was increased owing to molecular rearrangement and/or sintering at an interfacial region among crystalline monolayer domains (molecular creep).

Since Langmuir–Blodgett (LB) films prepared by transferring monolayers onto solid substrates provide the desired structure at a molecular level,[1,2] the LB films have been applied for various important functional characteristics, such as electric conductive,[2,3] photoelectrical,[4,5] and nonlinear optical properties.[6,7] For attainment of ultimate functional properties of LB films, construction of defect-diminished monolayers is required.[8] Analyses of the aggregation structure and mechanical properties of monolayers on the water surface may give an useful piece of information for construction of defect-diminished monolayers and LB films.

The aggregation structure of fatty acid monolayers on the water surface has been proposed on the basis of recent morphological and structural studies.[9—13] By transmission electron microscopic observations, fatty acid monolayers on the pure water surface was classified into a crystalline monolayer and an amorphous one at the subphase temperature (T_{sp}) below and above the melting temperature (T_m) of monolayer, respectively. These aggregation states were independent of the magnitude of the surface pressure. Therefore, it is apparent that the π–A isotherm for the fatty acid monolayer represents the gathering and packing processes of isolated domains grown right after spreading a solution on the water surface.[9,10]

Monolayers on the water surface frequently exhibit area-creep phenomena[14—24] for which the surface area decreases with time at a constant surface pressure. The area-creep phenomena of monolayers may be caused by the molecular relaxation in the monolayer domain, rearrangement of domains in the monolayer, and the collapse of the monolayer. Hence, the area-creep behavior of monolayers reflects the aggregation structure of the monolayer on the water surface.[15] Therefore, analysis of the relaxation mechanism of monolayers will give us a good information to construct the defect-diminished monolayer on the water surface.

The area-creep behavior of monolayers on the water surface has been discussed.[15—20] The area-creep of the stearic acid monolayer at various surface pressures was measured, which reported that the area decrement of monolayer on the area-creep measurement was not observed at the surface pressures below 10 mN m^{-1}.[16] The area-creep behavior of the stearic acid monolayer at various subphase pHs for $\pi=32.5$ mN m^{-1} was examined and reported that area losses at low and high pH were due to collapse of the monolayer, and dissolution into the subphase, respectively.[17] It was also reported that the monolayer should be collapsed by the area-creep at a high surface pressure and this collapse was caused by the mechanism of nucleation in the monolayer.[18—20] These results mentioned above were discussed on the basis only of mechanical properties of monolayer without any examination of the aggregation structure of the monolayer at the area-creep process. There were only a few morphological observations after the area-creep at a high surface pressure ($\geq$30 mN m^{-1}) where the monolayer was locally collapsed right after compression.[21,22]

In this study, the relaxation mechanism of the crystalline monolayer at various surface pressures on the water surface was investigated on the basis of area-creep measurements and transmission electron microscopic observations.

Experimental

Monolayer Preparation and Area-Creep Measure-

ment. Stearic acid (C_{18}, chromatographical reference quality) was used without further purification. A benzene with spectroscopic quality was used as solvent. Benzene solution of stearic acid was prepared with a concentration of 3.0×10^{-3} M (1 M=1 mol dm^{-3}) for a spreading solution. Subphase water was purified by the Milli-QII® system (Millipore Co., Ltd.). The sample solution was spread on the water surface at the subphase temperature (T_{sp}) of 293 K. Since this T_{sp} is below T_m and the crystalline relaxation temperature (T_{α_c}) of the stearic acid monolayer (T_m=317 K, T_{α_c}=298 K, evaluated from the static elasticity and ED pattern of monolayer),[9] the stearic acid monolayer on the water surface is in a crystalline state. The dimensions of the trough were 404 mm in length, 150 mm in width, and 5 mm in depth. The surface pressure was measured by the Wilhelmy method. Compression and area-creep measurements of the monolayer were operated with a micro processor-controlled film balance system (FSD-20, USI System Co., Ltd.). The monolayer was compressed at a constant rate of area change of 1.1×10^{-3} nm^2 molecule^{-1} s^{-1} until the desired surface pressure was attained. After compressing the monolayer, the variation of surface area of the monolayer was recorded for 4×10^4 s, while maintaining the monolayer at a constant surface pressure with a pressure variation of ±0.5 mN m^{-1}. The area-creep behavior of the monolayer was investigated by the time dependence of area strain. The area strain of the monolayer after area-creep for t s is obtained from Eq. 1.

$$\text{area strain } (t) = \{A(0) - A(t)\}/A(0) \qquad (1)$$

where $A(t)$ and $A(0)$ are the monolayer area at creep time t s and at the start of area-creep measurement, respectively.

Electron Microscopic Observation. The monolayer on the water surface was transferred onto a hydrophilic SiO substrate (static water contact angle: $\theta=30°$) where the monolayer could be transferred without any phase or crystallographical change.[9] The substrate was prepared by vapor-deposition of SiO onto a Formvar-covered electron microscope grid (200-mesh). The monolayer was transferred by the vertical dipping method at a transfer rate of 1.0 mm s^{-1}. Bright field electron micrographs and electron diffraction (ED) patterns were taken with a Hitachi H-7000 transmission electron microscope (TEM), which was operated at an acceleration voltage of 75 kV, a beam current of 0.5 μA and an electron beam spot size of 2 μm ϕ. TEM observations were carried out at a corresponding temperature to T_{sp} at which the monolayer was prepared. Pt–carbon was vapor-deposited onto the monolayer samples with a shadowing angle of 23° for the bright field electron micrographs.

Evaluation of Crystallographical Quality of Monolayer. Crystallographical quality of the monolayer was evaluated by means of the magnitude of crystallographical distortion (D_{lat}) and continuity (L_{lat}) in a direction along the monolayer surface, that is, the $hk0$ direction. D_{lat} corresponds to the root mean square value of differential rate between the positions of ideal crystalline lattice and real crystalline lattice, and L_{lat} the crystalline lattice length contributing to the electron diffraction coherency. These values were quantitatively evaluated by a modified single line method based on the Fourier analysis of ED profiles.[8,25—27]

Results and Discussion

Area-Creep Behaviors for Crystalline Monolayer of Stearic Acid at Various Surface Pressures. Figure 1 shows the area-creep curves for crystalline monolayer of stearic acid at T_{sp} of 293 K ($<T_{\alpha_c}<T_m$) under the surface pressures of 1, 5, 10, 15, and 24 mN m^{-1}. The area strains of the monolayers at 1, 5, and 10 mN m^{-1} increased gradually with creep time and almost remained constant after about 1×10^4 s. On the other hand, the area strains at 15 and 24 mN m^{-1} increased continuously even after about 1×10^4 s area-creep.

Figure 2 shows the bright field electron micrographs for the crystalline monolayer of stearic acid after 4×10^4 s area-creep at 10 and 15 mN m^{-1} at 293 K. The bright field micrograph at 10 mN m^{-1} (Fig. 2(a)) showed that the monolayer was morphologically homogeneous, while the monolayer was inhomogeneous at 15 mN m^{-1}, as shown in Fig. 2(b). Since the monolayers right after compression to 10 and 15 mN m^{-1} were morphologically homogeneous, the inhomogeneous morphology of the monolayer at 15 mN m^{-1} area-creep (Fig. 2(b)) might be due to collapse of the monolayer during an

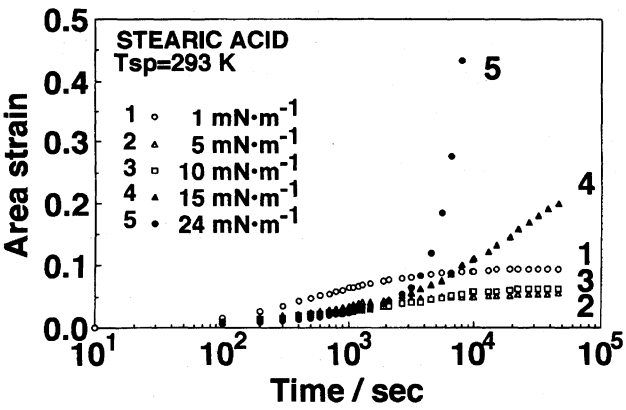

Fig. 1. Area-creep curves for crystalline monolayer of stearic acid at various surface pressures at 293 K.

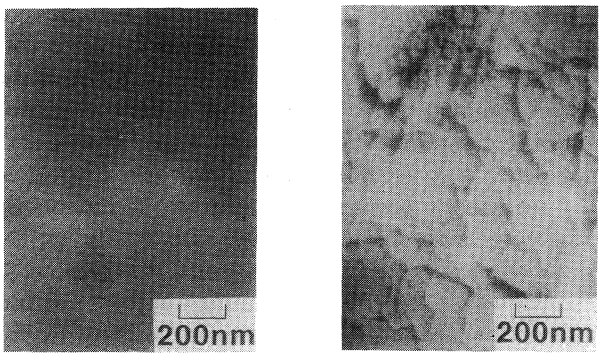

(a) 10 mN m^{-1} (b) 15 mN m^{-1}

Fig. 2. Bright field electron micrographs of stearic acid monolayer after 4×10^4 s area-creep at (a) 10 mN m^{-1}, (b) 15 mN m^{-1}.

area-creep process.

Thus, the area-creep behavior for the crystalline monolayer of stearic acid depends on the magnitude of surface pressure and is principally classified into the behaviors at high ($\geq$15 mN m^{-1}) and low ($\leq$10 mN m^{-1}) surface pressure regions in the case of T_{sp} of 293 K.

Area-Creep Behavior at High Surface Pressures ($\geq$15 mN m^{-1}). Figure 3 shows the area-creep curve for the crystalline monolayer of stearic acid at 293 K and at 24 mN m^{-1} where the monolayer right after compression was morphologically homogeneous,[9,10] and the bright field electron micrographs of the monolayers at creep times of 60, 7×10^2, and 2×10^3 s. The area strain of the monolayer at a creep time shorter than about 1×10^2 s increased almost linearly with creep time and the increment of area strain was small, whereas the area strain at a creep time longer than around 1×10^2 s increased remarkably. Thus, the area-creep behavior of the monolayer at 24 mN m^{-1} was roughly classified into the area-creep behaviors in shorter and longer time regions than the creep time of 1×10^2 s. The electron micrograph at the creep time of 60 s showed that the monolayer was still morphologically homogeneous. In contrast, the electron micrographs at the creep times of 7×10^2 and 2×10^3 s showed that the monolayer was heterogeneous owing to collapse of the monolayer. Therefore, the remarkable increment of area strain in the long time region may be attributed to collapse of the monolayer. In the case of T_{sp} below T_{α_c}, the isolated two-dimensional crystalline domains are formed right after spreading a solution. With compression of monolayer, these crystalline domains are gathered together into morphologically homogeneous, with alignment of their crystallographic axes, owing to the sintering at interfacial region among crystalline domains.[9,10] Since sintering among the crystalline domains takes a fairly long time, the compression studied in Fig. 3 was insufficient to form a large homogeneous monolayer.[9,21] Then, the vacancies among crystalline domains were still remained in the monolayer, even though compression was carried out up to such high surface pressure (24 mN m^{-1}) with the constant rate of compression (120 mm^2 s^{-1}). Therefore, it seems reasonable to consider that the sintering among the crystalline domains are so incomplete that vacancies at a molecular level among the crystalline domains still remain. Since such a monolayer is structurally inhomogeneous, a compression force cannot propagate equally in the monolayer. In this case, high surface pressure is partially applied in the monolayer. From above reasons, it is reasonable to conclude that the collapse at a high surface pressure in a long time area-creep may be easily induced by this partial stress concentration, as shown by the electron micrographs at a long time area-creep. On the other hand, it is clear from the homogeneous morphology of the monolayer as shown in Fig. 3 that the area-creep behavior in a short time region is not due to the collapse of monolayer.

In order to clarify the area-creep mechanism of the crystalline monolayer at a high surface pressure in a short time region, the area-creep behavior was discussed on the basis of the relationship between area strain and elasticity of the monolayer. Static elasticity, K_s of monolayer was evaluated by the derivative of π with respect to A, $-A(d\pi/dA)$.[9] The various types of aggregation structure of monolayers have been reported on the basis of lower or higher T_{sp} with respect to T_{α_c} and T_m of monolayers.[9,28] In these studies, the maximum of K_s ($K_{s(max)}$) was used as a characteristic mechanical value for the monolayer being composed of assembly of crystalline domains in the monolayer. Figure 4 shows the relationship between the area strain and log $K_{s(max)}$ of the various monolayers. The area strains of the myristic (C_{14}, T_{sp}=293 K$>T_m$=278 K), palmitic (C_{16}, T_{α_c}=291 K$<T_{sp}<T_m$=301 K), and stearic (C_{18}, $T_{sp}<T_{\alpha_c}$=298 K$<T_m$=317 K) acid monolayers at 1×10^2 s upon the area-creep measurements were measured at the surface pressures where the each monolayer was morphologically homogeneous (C_{14}: 14 mN m^{-1}, C_{16}: 20 mN m^{-1}, C_{18}: 24 mN m^{-1}). Also the results for the palmitic acid monolayers at T_{sp}s of 288 K ($T_{sp}<T_{\alpha_c}$) and 306 K ($T_{sp}>T_m$) were shown in Fig. 4.

As previously reported,[28] the molecular aggregation in the monolayer on the water surface was different depending on T_{sp}, pH, alkyl chain length of fatty acid molecule and so on, that in fusing-oriented crystalline monolayer, randomly assembled crystalline monolayer and amorphous monolayer. The relationship between the area strain and log $K_{s(max)}$ shown in Fig. 4 apparently indicates that the area-creep behavior of the monolayer in a short time region as shown in Fig. 3 is strongly related to the molecular rearrangement, which is the change of molecular position or molecular orientation, rather than the geometrical restructuring such as disappearance of voids or interfaces. Therefore, it is reasonable to conclude that the area-creep behavior of the monolayer in a short time region at a high surface pressure results from the rearrangement of molecules in the crystalline domain.

Area-Creep Behavior at Low Surface Pressures ($<$10 mN m^{-1}). Figure 1 showed that the area strain at 10 mN m^{-1} became constant after about 1×10^4 s area-creep where the monolayer morphology was homogeneous as shown in Fig. 2. This indicates that the area-creep behavior for the crystalline monolayer of stearic acid at a low surface pressure is not due to collapse of the monolayer. Hence, it is reasonable to consider that the area-creep behavior of the monolayer might be caused by filling the vacancies among the crystalline domains with molecules or the molecular rearrangement in the crystalline domain of monolayer.

Figure 5 shows the molecular occupied area with time during the area-creep for the crystalline monolayer of stearic acid at 293 K. The molecular occupied area

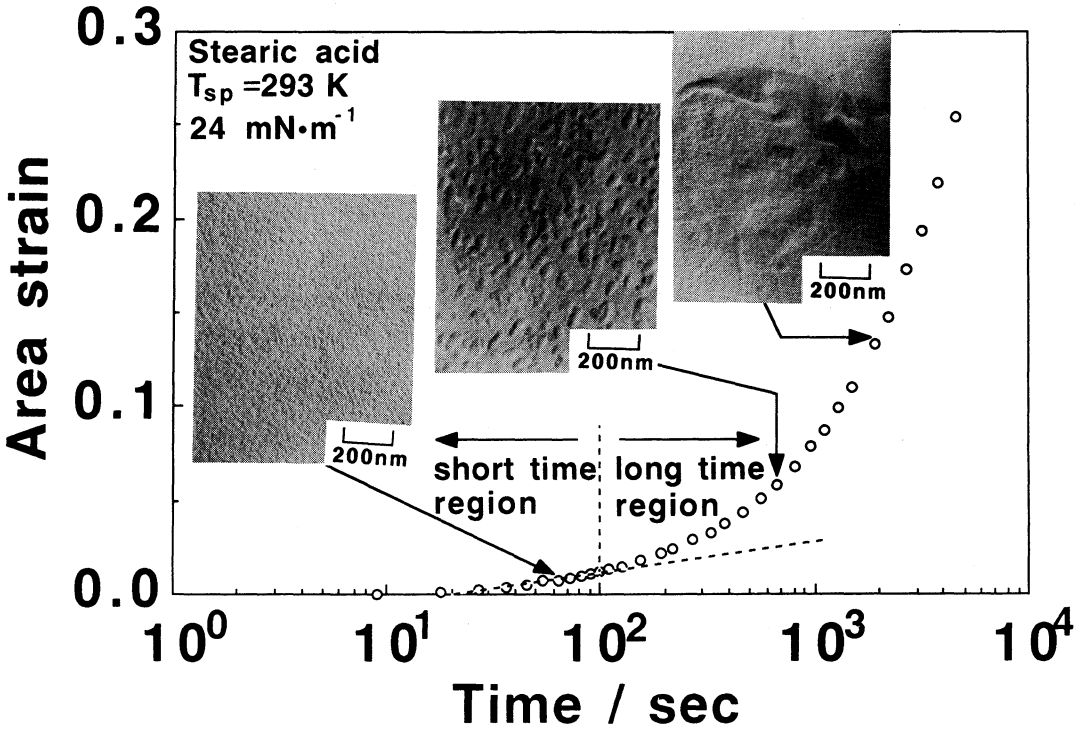

Fig. 3. Area-creep curve for crystalline monolayer of stearic acid at 24 mN m^{-1}, at 293 K, and the bright field images of monolayer.

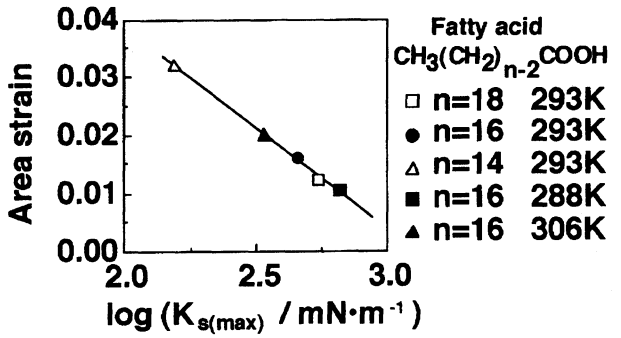

Fig. 4. Relationship between the log $K_{s(max)}$ and the area strain of fatty acid monolayers at the creep time of 1×10^2 s and at T_{sp} of 293 K.

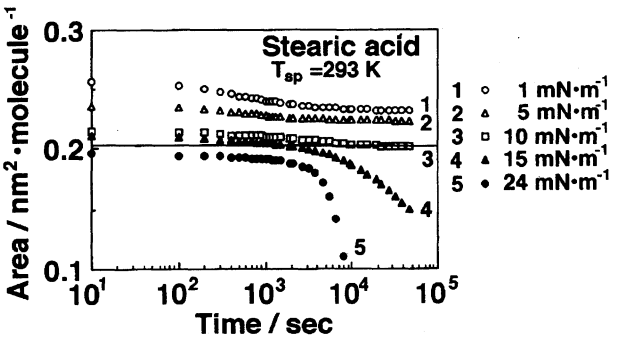

Fig. 5. Change of molecular occupied area during area-creep for crystalline monolayer of stearic acid at various surface pressures at 293 K.

corresponds to A of the π–A isotherm. The straight line in Fig. 5 represents the molecular occupied ares, A_{calcd} calculated on the basis of the ED pattern of the stearic acid monolayer being transferred onto the substrate at 10 mN m^{-1} at 293 K. Since stearic acid molecules in the monolayer are packed in a hexagonal unit cell at T_{sp} of 293 K, the magnitude of A_{calcd} can be calculated from (10) spacing, d_{10} by Eq. 2

$$A_{calcd} = 2 \times \left(3^{-1/2}\right) (d_{10})^2 \qquad (2)$$

The molecular occupied area just after compression to 10 mN m^{-1} was larger than A_{calcd}. The area decrement of the monolayer at 10 mN m^{-1} was about 6 % of the initial area at the start of area-creep. This magnitude of area decrement was so large that it is considered that this may not arise only from the molecular rearrangement but the decrement of the area of vacancies among crystalline domains. The molecular occupied area at 10 mN m^{-1} became comparable to the calculated molecular occupied area after about 1×10^4 s area-creep where the monolayer morphology was still homogeneous with a TEM observation level. Since the crystalline lattice spacing of the stearic acid monolayer was constant during the area-creep at 10 mN m^{-1}, it is reasonable to consider that the area decrement for the crystalline monolayer of stearic acid arises mainly from decrement of the area of vacancies among the crystalline domains in the monolayer.

Table 1 shows the variations of crystallographical distortion (D_{lat}) and continuity (L_{lat}) for the crystalline monolayer of stearic acid during the area-creep measurement at 10 mN m^{-1} at 293 K. The magnitude of D_{lat}

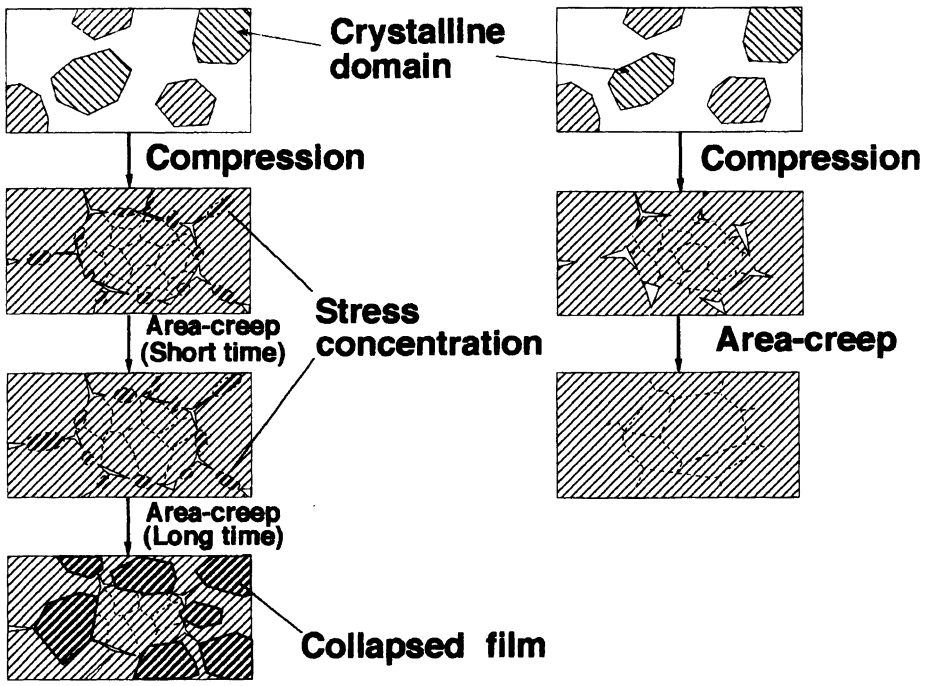

(a) High surface pressure (b) Low surface pressure

Fig. 6. Schematic representation of aggregation structure of the crystalline monolayer during area-creep at (a) high and (b) low surface pressures.

Table 1. Variations of Crystallographical Distortion and Continuity of Stearic Acid Crystalline Monolayers in Area-Creep Measurement at 293 K, 10 $mN\,m^{-1}$

Creep time / s	Crystallographical distortion, D_{lat}/%	Crystallographical continuity, L_{lat}/nm
0	5.4	4.6
1×10^4	4.3	8.8
4×10^4	3.9	10.9

decreased and that of L_{lat} increased with creep time. This indicates that crystallographical regularity on the basis of the magnitudes of D_{lat} and L_{lat} of the stearic acid monolayer is progressed during the area-creep at 10 $mN\,m^{-1}$ at 293 K, probably because of sintering among the crystalline domains under the experimental condition at T_{sp} below T_{α_c}.[9,15] Hence, it can be considered that the rearrangement of the stearic acid molecules in the crystalline domain is also one of the main causes of the area decrement of monolayer during area-creep at a low surface pressure. Consequently, it is reasonable to conclude from Figs. 2 and 5 and Table 1 that the vacancies among crystalline domains in the stearic acid monolayer are filled up with fatty acid molecules and also the crystallographical regularity of the monolayer is progressed during the area-creep at 10 $mN\,m^{-1}$.

The Area-Creep Model on Aggregation Structure of Monolayer. Figure 6 shows the schematic representation for change of the aggregation structure in the crystalline monolayer of stearic acid during the area-creep at a high surface pressure (a) and a low one (b). In Fig. 6, straight and dotted lines in the crystalline domain show crystallographic orientation and crystallite boundary, respectively. The monolayer crystallite means the crystal without any crystallographical defect, and therefore, the size of the crystallite is equal to L_{lat} being evaluated by the single line method.[25] At T_{sp} below T_{α_c}, crystalline domains are formed even though at 0 $mN\,m^{-1}$, right after spreading a sample solution on the water surface.[9,10] With compressing the monolayer crystalline domains at a constant speed to a high surface pressure (Fig. 6(a)), the crystalline domains were gathered together, aligning their crystallographic axes owing to sintering among the crystalline domains.[9] However, some vacancies among the crystalline domains were still remained by compression at a constant speed to a high surface pressure as shown in Fig. 6(a). It seems reasonable to consider that vacancies were remained by aggregation-structural fixation induced by a continuous compression up to a high surface pressure. The existence of vacancies in general, causes a stress concentration around them in the monolayer, resulting in collapse of monolayer by the long time area-creep at a high surface pressure.

On the other hand, after compression of monolayer to a low surface pressure (Fig. 6(b)), vacancies among the crystalline domains also exist inducing stress concentration. However, it can be considered that the surface pressure of monolayer is so low that the magnitude of stress concentration may be insufficient to collapse the monolayer. Hence, the collapse of monolayer does not

occur at a low surface pressure even after the long time area-creep. The area of vacancies among the crystalline domains decreases and crystallites in the crystalline domains grow to be a larger one owing to sintering at the domain interface during the area-creep of the monolayer at a low surface pressure. Therefore, the area-creep at a low surface pressure is considered to be one way to prepare the defect-diminished monolayer.

Conclusion

The area-creep mechanism for the crystalline monolayer of stearic acid was classified into two regions based on the area-creep behaviors at the different magnitudes of surface pressures. At a high surface pressure, the monolayer collapsed owing to a stress concentration around the vacancies upon the area-creep for a long time, although molecules in the crystalline domain were rearranged during the area-creep for the short time. On the other hand, at a low surface pressure, the area of the vacancies among the crystalline domains decreased, and also the crystallographical regularity of the monolayer was remarkably progressed. Then, the area-creep behavior at a low surface pressure suggests us how to prepare the defect-diminished monolayer.

References

1) K. B. Blodgett, *J. Am. Chem. Soc.*, **56**, 1007 (1935).
2) B. Tieke, *Adv. Mater.*, **2**, 222 (1990).
3) J. Anzai and T. Osa, *Sel. Electrode Rev.*, **12**, 3 (1990).
4) Y. L. Hua, D. P. Jiang, Z. Y. Shu, M. C. Petty, G. G. Roberts, and M. M. Ahmad, *Thin Solid Films*, **192**, 383 (1990).
5) E. Brynda, L. Kalvoda, I. Koropecky, S. Nespurek, and J. Rakusan, *Synth. Met.*, **37**, 327 (1990).
6) N. J. Geddes, M. C. Jurich, J. D. Swalen, R. Twieg, and J. F. Rabolt, *J. Chem. Phys.*, **94**, 1603 (1991).
7) H. Fuchs, H. Ohst, and W. Prass, *Adv. Mater.*, **3**, 10 (1991).
8) E. Yuda, M. Uchida, Y. Oishi, and T. Kajiyama, *Rep. Prog. Polym. Phys. Jpn.*, **32**, 151 (1989).
9) T. Kajiyama, Y. Oishi, M. Uchida, N. Morotomi, J. Ishikawa, and Y. Tanimoto, *Bull. Chem. Soc. Jpn.*, **65**, 864 (1992).
10) T. Kajiyama, Y. Oishi, M. Uchida, Y. Tanimoto, and H. Kozuru, *Langmuir*, **8**, 1563 (1992).
11) N. Uyeda, T. Takenaka, K. Aoyama, M. Matsumoto, and Y. Fujiyoshi, *Nature*, **327**, 319 (1987).
12) B. G. Moore, C. M. Knobler, S. Akamatsu, and F. Rondelez, *J. Phys. Chem.*, **94**, 4588 (1990).
13) D. Honig, G. A. Overbeck, and D. Mobius, *Adv. Mater.*, **4**, 419 (1992).
14) G. L. Gaines, Jr., "Insoluble Monolayers at Liquid–Gas Interfaces," Interscience, New York (1966), Chap. 4.
15) T. Kuri, Y. Oishi, and T. Kajiyama, *Rep. Prog. Polym. Phys. Jpn.*, **35**, 347 (1992).
16) R. D. Smith and J. C. Berg, *J. Colloid Interface Sci.*, **74**, 273 (1980).
17) R. Aveyard, B. P. Binks, N. Carr, and A. W. Cross, *Thin Solid Films*, **188**, 361 (1990).
18) D. Vollhardt and U. Retter, *J. Phys. Chem.*, **95**, 3723 (1991).
19) D. Vollhardt, U. Retter, and S. Siegel, *Thin Solid Films*, **199**, 189 (1991).
20) D. Vollhardt and U. Retter, *Langmuir*, **8**, 309 (1992).
21) T. Tanizaki, A. Takahara, and T. Kajiyama, *J. Soc. Rheol., Jpn.*, **19**, 208 (1991).
22) R. D. Neuman, *J. Colloid Interface Sci.*, **56**, 505 (1976).
23) K. Sakai, T. Kuwabara, M. Imamura, E. Ohta, T. Sato, and M. Sakata, *Hyomen Kagaku*, **14**, 265 (1993).
24) T. Kato, K. Ohshima, and K. Suzuki, *Thin Solid Films*, **178**, 37 (1989).
25) D. Hofmann and E. Walenta, *Polymer*, **28**, 1271 (1987).
26) T. Kajiyama, I. Hanada, K. Shuto, and Y. Oishi, *Chem, Lett.*, **1989**, 193.
27) T. Kajiyama, K. Umemura, M. Uchida, Y. Oishi, and R. Takei, *Chem. Lett.*, **1989**, 1515.
28) T. Kajiyama, Y. Oishi, M. Uchida, and Y. Takashima, *Langmuir*, **9**, 1978 (1993).